Molecular Microbiology (2010) 76(2), 331–347 ■
doi:10.1111/j.1365-2958.2010.07100.x
First published online 10 March 2010

Complex interplay between the LysR-type regulator AtzR and its binding site mediates *atzDEF* activation in response to two distinct signals

Odil Porrúa,[1,2†] Ana Isabel Platero,[1,2] Eduardo Santero,[1,2] Gloria del Solar[3] and Fernando Govantes[1,2*]

[1]*Centro Andaluz de Biología del Desarrollo, Universidad Pablo de Olavide/CSIC. Carretera de Utrera, Km. 1. 41013 Sevilla, Spain.*

[2]*Departamento de Biología Molecular e Ingeniería Bioquímica, Universidad Pablo de Olavide. Carretera de Utrera, Km. 1. 41013 Sevilla, Spain.*

[3]*Department of Protein structure and function. Centro de Investigaciones Biológicas, CSIC. Ramiro de Maeztu 9, 28040 Madrid, Spain.*

Summary

AtzR is a LysR-type regulator responsible for activation of the cyanuric acid utilization operon *atzDEF*. AtzR binds the P*atzDEF* promoter region at a strong recognition element, designated the repressor binding site, and a weaker binding determinant, the activator binding site (ABS). AtzR activates transcription in response to two dissimilar signals, nitrogen limitation and cyanuric acid. In the present work we analyse the structure and function of the *cis*-acting elements involved in AtzR activation of *atzDEF*. Hydroxyl radical footprinting assays revealed that the ABS is composed of three functional subsites spaced at one helix-turn intervals. Two modes of interaction with the ABS are detected *in vitro*: AtzR binds at the ABS-2 and ABS-3 subsites in the absence of inducer, and relocates to interact with the ABS-1 and ABS-2 subsites in the presence of cyanuric acid. *In vivo* mutational analysis indicates that ABS-1 and ABS-2 are required for full P*atzDEF* activation in all conditions. In contrast, ABS-3 acts as a 'subunit trap' that hinders productive AtzR interactions with ABS-1 and ABS-2. Our results strongly suggest an activation model in which cyanuric acid and nitrogen limitation cooperate to reposition AtzR from an inactive, ABS-3 bound configuration to an active, ABS-1- and ABS-2-bound configuration.

Accepted 15 February, 2010. *For correspondence. E-mail fgovrom@upo.es; Tel. (+34) 954977877; Fax (+34) 954349376. †Present address: LEA Laboratory of Nuclear RNA metabolism, Centre de Génétique Moléculaire, Centre National de la Recherche Scientifique – UPR2167. 1, Av de la Terrasse, 91190, Gif sur Yvette, France.

Introduction

LysR-type transcriptional regulators (LTTRs) represent the most abundant family of transcriptional regulatory proteins in bacteria. LTTRs typically activate transcription in response to a small molecule that acts as an inducer. Genes encoding LTTRs are often divergently transcribed from the activated genes and their expression is negatively autoregulated. In these cases, activation and autorepression are exerted from a single asymmetrical binding site located within the divergent promoter region. LTTR binding sites contain a palindromic recognition element, harbouring the conserved T-N_{11}-A motif, designated the repressor binding site or RBS. The RBS is normally centred at position –65 relative to the activated promoter transcriptional start, and often overlaps the repressed promoter. The RBS is considered the major sequence determinant for LTTR DNA binding and is required for both activation and repression. A second sequence element, the activator binding site or ABS, is located in the vicinity of the –35 element of the activated promoter. The ABS has no conserved structure, but it has been shown to bear some resemblance to the RBS sequence in several cases. Despite the fact that the ABS is generally recognized to play a minor role in DNA binding, it is essential for activation. Studies on transcriptional activation by several members of the LTTR family have revealed many mechanistic details, and a general model for inducer-dependent activation, the 'sliding dimer' model, has been proposed. According to this model, LTTRs bind DNA as tetramers, with two subunits interacting with the RBS and two subunits interacting with the ABS. This mode of binding induces a sharp bend in the DNA strand. In the presence of their inducers, LTTRs undergo a rearrangement that repositions the two ABS-bound subunits. Such rearrangement shifts the LTTR–DNA complex from an extended conformation to a more compact conformation, relaxing the induced DNA bend and allowing productive interactions between the

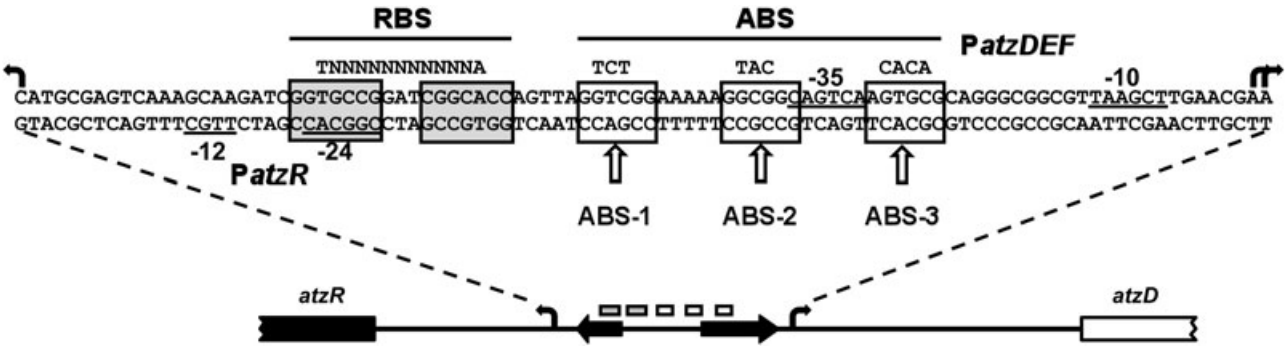

Fig. 1. Schematic of the P*atzDEF* activation binding site (ABS). The *atzR* and *atzD* coding sequences are indicated by broken boxes. Promoters and transcription start sites are shown as solid and bent arrows, respectively, and shaded and open boxes denote the RBS half-sites and the ABS subsites respectively. The highlighted sequence shows features of the AtzR binding site region. P*atzR* and P*atzDEF* conserved promoter motifs are underlined, and the identity of the ABS-1, ABS-2 and ABS-3 substitutions are indicated above the sequence.

regulator and the RNA polymerase (reviewed by Schell, 1993; Tropel and van der Meer, 2004; Maddocks and Oyston, 2008).

AtzR is a LTTR that activates the expression of the divergently transcribed cyanuric acid degradative operon *atzDEF* of *Pseudomonas* sp. ADP in response to cyanuric acid and nitrogen limitation. AtzR is a cyanuric acid sensor (Porrúa *et al*., 2007) that also responds to a nitrogen limitation signal transduced by the PII protein GlnK (García-González *et al*., 2009). Expression of *atzR* is subjected to positive control by the global regulator NtrC in response to nitrogen limitation and is repressed by its own gene product in a cyanuric acid-independent fashion (García-González *et al*., 2005; Porrúa *et al*., 2009). The *atzR–atzDEF* regulatory circuit has been reviewed recently elsewhere (Govantes *et al*., 2009).

Our previous work showed that the architecture of the AtzR binding site within the *atzR–atzDEF* divergent promoter region matches the typical organization of LTTR binding sites (Porrúa *et al*., 2007). It harbours a RBS containing the T-N_{11}-A motif centred in position –65 relative to the *atzDEF* transcriptional start and an ABS overlapping the –35 element of P*atzDEF* (Fig. 1). The RBS is a strong AtzR binding site, required for high-affinity binding of AtzR, P*atzDEF* activation and autorepression (Porrúa *et al*., 2007). The functional organization of the ABS is unknown, but the presence of three hexameric motifs, designated ABS-1, ABS-2 and ABS-3, whose sequences partially resemble the RBS sequence has been noted (Fig. 1) (Porrúa *et al*., 2007). Our previous results on the effect of cyanuric acid on the interaction of AtzR with its binding site are consistent with the 'sliding dimer' model (Porrúa *et al*., 2007). Accordingly, AtzR induces a bend in the DNA molecule upon binding, and cyanuric acid triggers a conformational change of the AtzR–DNA complex characterized by a relaxation of the induced DNA bend and a shortening of the DNase I footprint at the ABS (Porrúa *et al*., 2007). In addition, we have recently shown that the contribution of the ABS to AtzR binding affinity is required for autorepression both *in vivo* and *in vitro* (Porrúa *et al*., 2009).

In the present work, we set out to analyse the fine structure of the ABS at the *atzR–atzDEF* promoter region and its function in AtzR-dependent activation of the P*atzDEF* promoter. Our data indicate that the ABS is a tripartite sequence element in which individual subsites have distinct roles in the activation process. We propose a model in which the relative affinity of AtzR for the ABS subsites and the presence or absence of inducing conditions govern the formation of two different AtzR–DNA complexes: an extended, inactive complex and a compact complex that is competent for transcriptional activation.

Results

AtzR binds DNA on one side of the DNA helix to contact the ABS-1, ABS-2 and ABS-3 subsites

In order to obtain a detailed picture of the contacts of AtzR with the DNA backbone at its binding site, hydroxyl radical footprinting assays were performed using AtzR-His_6 and the wild-type *atzR–atzDEF* promoter region as a probe, both in the presence and in the absence of cyanuric acid. The results are depicted in Figs 2 and 3.

In the absence of cyanuric acid, AtzR protected six groups of two to four nucleotides around positions –21, –32, –42, –53, –63 and –74 at the top strand, and –25, –35, –46, –56, –67 and –76 at the bottom strand (coordinates are relative to the *atzDEF* transcriptional start throughout) (Figs 2A and C and 3A). These clusters of protected positions occur with approximately one helical turn periodicity, strongly suggesting that AtzR binds DNA on one side of the helix. This protection pattern defines five groups of 3–4 bp that are not protected in either strand and are flanked by protected positions. When modelled on a DNA helix projection (Fig. 3A), these five

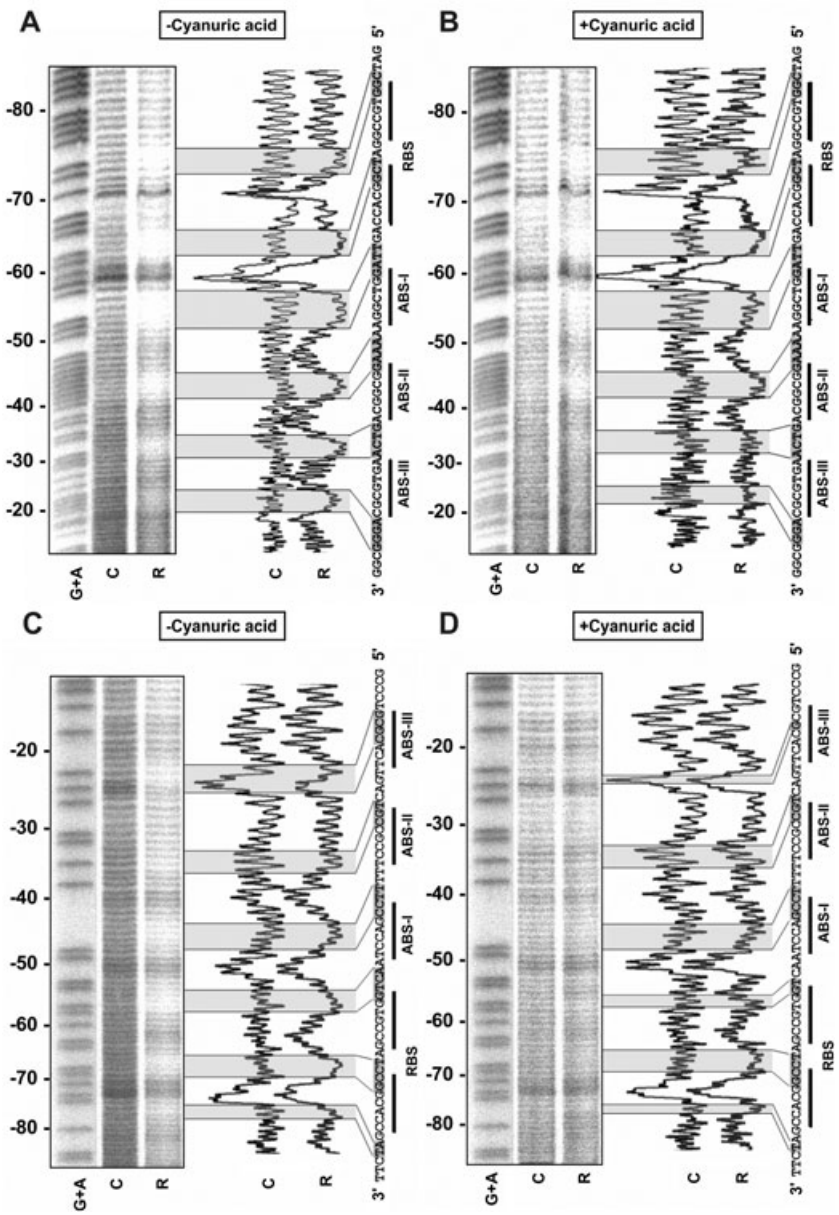

Fig. 2. High-resolution mapping of AtzR interaction with its binding site by hydroxyl radical footprintings.
A and B. Top strand in the absence and in the presence of cyanuric acid respectively.
C and D. Bottom strand in the absence and in the presence of cyanuric acid respectively.
Gel pictures show the cleavage pattern of the probe in the absence (C) and in the presence of AtzR (R). To facilitate visualization of protections, the quantification curve of each lane is shown on the right of each panel, along with the sequence of the strand analysed. Co-ordinates relative to the P*atzDEF* transcriptional start are displayed on the left side of each panel. Protected positions are indicated in the sequence by shaded boxes, and the sequences of the proposed RBS and ABS motifs are denoted by solid lines. Differences in the extent of protection are not shown (see Fig. 3).

groups correspond to bases exposed in five consecutive major grooves at the face of the helix bound by AtzR. As LTTRs interact with bases exposed at the major groove (Maddocks and Oyston, 2008), these are likely targets for sequence-specific recognition by the regulatory protein. The five groups of exposed base pairs largely overlap with the RBS half-sites and the proposed ABS subsites (Porrúa *et al*., 2007). The protection pattern obtained is consistent with interaction of the AtzR tetramer with the two external major grooves and two of the three internal major grooves within the protected region. Based on the similarity of these results with those previously shown for other LTTRs (Toledano *et al*., 1994; Hryniewicz and Kredich, 1995; Wang and Winans, 1995a), and the predictions derived from the crystal structure of CbnR (Muraoka *et al*., 2003), we propose that, in the absence of cyanuric acid, the central ABS-1 subsite remains free, while two AtzR monomers interact with the RBS half-sites, and the other two are bound to the ABS-2 and ABS-3 subsites.

In the presence of cyanuric acid, the hydroxyl radical footprinting pattern exhibited minor changes in the extent of protection in a few positions around the RBS and the ABS-1 and ABS-2 subsites (Fig. 3B). However, the most salient feature was a strong decrease in protection for all the positions flanking the ABS-3 subsite that were protected in the absence of cyanuric acid. At the top strand, protection was not detected at position –19 and was

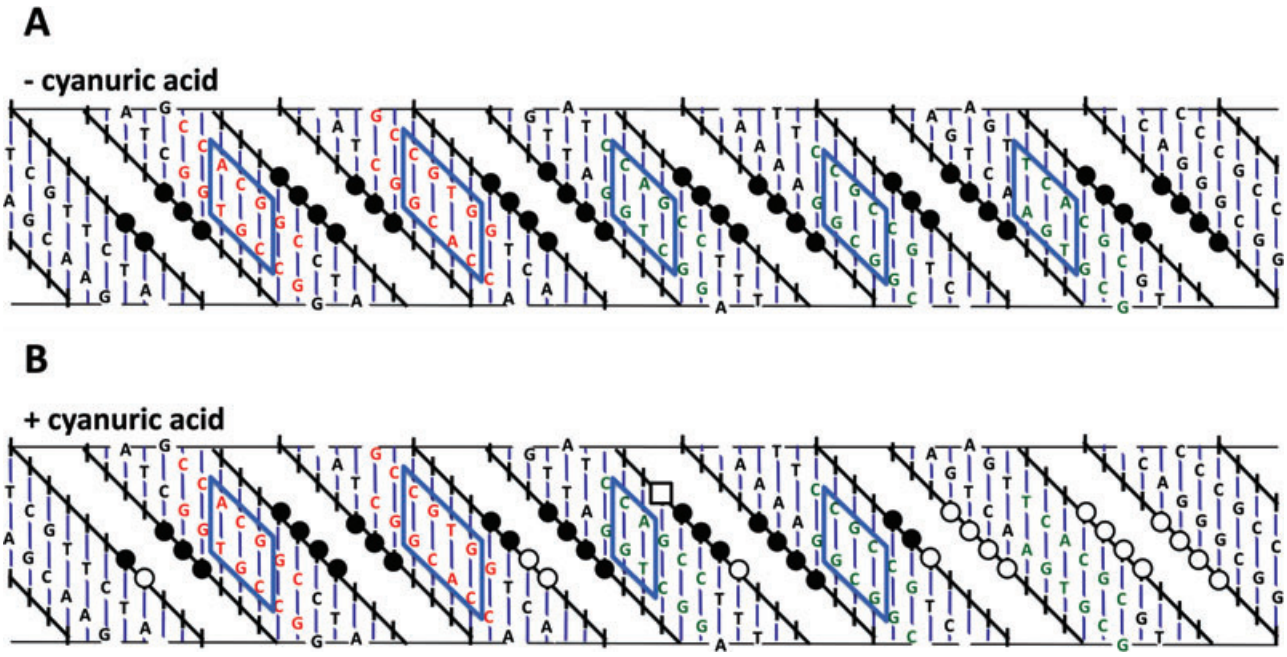

Fig. 3. Helical projection of the positions protected from hydroxyl radical cleavage. The DNA helix is modelled as a cylinder surface cut longitudinally. Solid black lines denote the sugar-phosphate backbone, with markers indicating the insertion of the bases. Positions of the base pairs are shown along the major groove. The helix pitch is 10.5 bp per helix turn.
A. Data from the hydroxyl radical footprint performed in the absence of cyanuric acid. Closed circles denote the protected positions.
B. Data from the hydroxyl radical footprint performed in the presence of cyanuric acid. Closed circles: positions similarly protected in the presence and in the absence of cyanuric acid. Open circles: positions with significantly decreased protection in the presence of cyanuric acid. Open squares: positions displaying increased protection in the presence of cyanuric acid. Bases corresponding to the proposed RBS and ABS motifs are denoted by red and green colour respectively. Blue diamonds denote unprotected base pairs exposed in the major groove facing AtzR.

greatly diminished at positions –20, –21, –22, –30, –31, –32 and –33. At the bottom strand, positions –23, –24 and –26 were unprotected, while protection at position –25 was significantly reduced (Figs 2 and 3). These results strongly suggest that, in the presence of the inducer, AtzR adopts a more compact conformation at its binding site that precludes contacts with ABS-3. Thus, in this configuration, the AtzR tetramer is most likely positioned on the RBS and the two RBS-proximal subsites ABS-1 and ABS-2. Taken together, these results strongly support the hypothesis that the ABS has a tripartite structure, and are fully consistent with the 'sliding dimer' model as previously described (Porrúa *et al*., 2007).

Mutational analysis of the ABS in vivo

As the *in vitro* hydroxyl radical footprinting assays lend support to the proposed three-subsite structure of the ABS, we aimed to test the roles of the different subsites within the ABS in AtzR-mediated activation of *atzDEF in vivo*. To achieve this goal, each of the ABS subsites was modified by site-directed mutagenesis (Fig. 1). The mutations were designed to impair the positions likely involved in sequence-specific AtzR contacts, and decrease the resemblance with the RBS sequence. Plasmids pMPO144, pMPO148 and pMPO150 harbour *atzD–lacZ* translational fusions with the mutant subsites ABS-1, ABS-2 and ABS-3, respectively, while plasmids pMPO169, pMPO170 and pMPO171 bear combinations of the ABS-1 and ABS-2, ABS-1 and ABS-3, and ABS-2 and ABS-3 mutant subsites respectively. These plasmids were transferred, along with the wild-type promoter fusion plasmid pMPO202, to *Pseudomonas putida* KT2442 by mating. KT2442 is a genetically tractable model *Pseudomonas* strain that we have routinely used as a surrogate host for gene expression studies in this system (García-González *et al*., 2005; Porrúa *et al*., 2007; 2009). The effects of these substitutions on *atzDEF* expression were tested by means of β-galactosidase assays in the presence and in the absence of the AtzR-producing plasmid pMPO109 (Fig. 4).

In the absence of AtzR, expression of *atzDEF* was similar in all fusions (*c.* 200–300 Miller units), indicating that integrity of the ABS motifs is not required for basal, AtzR-independent transcription (data not shown). The behaviour of the wild-type fusion in the presence of AtzR was as previously described (García-González *et al*., 2005). Accordingly, basal expression levels were observed in nitrogen excess, which were increased

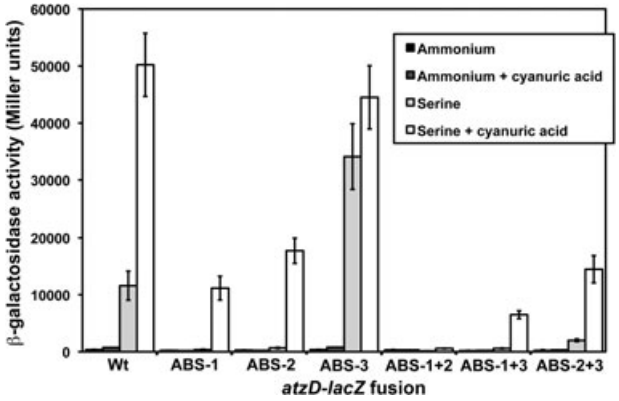

Fig. 4. Expression of *atzD–lacZ* translational fusions containing mutations at the ABS subsites in *P. putida* KT2442 containing the AtzR-producing plasmid pMPO109. Values are β-galactosidase activity (Miller units). Bars represent the average of at least three independent measurements and error bars denote the standard deviation for each set of assays.

twofold by the presence of cyanuric acid. In nitrogen-limited medium, expression was induced 33-fold in the absence and 143-fold in the presence of cyanuric acid, relative to the basal levels. The *atzD*–ABS-1 and *atzD*–ABS-2 fusions showed similar phenotypes in all growth media. Activation in response to either cyanuric acid or nitrogen limitation was abolished, suggesting that interaction of AtzR with the mutated subsites is critical for activation in these conditions. In contrast, expression levels of the *atzD*–ABS-1 and *atzD*–ABS-2 fusions were only reduced five- and fourfold relative to the wild-type construct when both activating signals concurred, and high levels of activation (35- and 50-fold respectively) were still observed. The *atzD*–ABS1+2 fusion, containing both ABS-1 and ABS-2 mutant subsites, showed basal expression levels under all conditions. These results indicate that interaction of AtzR with ABS-1 and ABS-2 is required for full activation under all conditions tested. However, while integrity of ABS-1 and ABS-2 is strictly required for activation in response to either nitrogen limitation or cyanuric acid, in the presence of both signals, AtzR can activate P*atzDEF* to relatively high levels when only one of these subsites is intact. The *atzD*–ABS-3 fusion exhibited wild-type expression levels in all conditions except in nitrogen-limited medium lacking cyanuric acid, in which expression was increased threefold, to levels comparable to those in the presence of both activating signals. Combination of the ABS-3 and ABS-1 mutations resulted in a phenotype similar to that of the single ABS-1 mutant. Activation in response to cyanuric acid or nitrogen limitation alone was abolished and the expression levels in the presence of both signals were diminished, albeit the effect in the latter conditions was slightly (twofold) greater in the double mutant. The *atzD*–ABS-2+3 fusion, harbouring mutations at the ABS-2 and ABS-3 subsites, behaved similarly to the single ABS-2 mutant, except that it retained partial activation (eightfold) in response to nitrogen limitation. These results indicate that integrity of ABS-3 is not required for P*atzDEF* activation. Instead, ABS-3 plays a negative control role that is apparent in nitrogen-limited medium lacking cyanuric acid. Integrity of the ABS-1 and ABS-2 subsites is required for overactivation of the P*atzDEF* promoter in nitrogen limitation conditions due to the ABS-3 mutation, although only recognition of the former appears to be critical. Finally, the lack of effect of the ABS-3 mutation in the presence of both signals suggests that interaction with the ABS-3 subsite does not occur in these conditions.

We have previously shown that AtzR represses the P*atzR* promoter by competing with σ^{54}-bearing RNA polymerase for their overlapping binding sites. A deletion encompassing most of the ABS prevented autorepression, indicating that the contribution of the ABS region to AtzR binding is critical to this process (Porrúa *et al.*, 2009). As a means to probe the interaction of AtzR with the ABS subsites *in vivo* further, we aimed to test the effect of the ABS subsite mutations on P*atzR* repression. With this purpose, plasmids pMPO104, pMPO145, pMPO149 and pMPO151, harbouring *atzR–lacZ* fusions to the wild type and the mutant ABS-1, ABS-2 and ABS-3 promoter regions, respectively, were constructed and transferred to *P. putida* KT2442. Expression was measured as β-galactosidase activity, as described above. The results are shown in Table 1.

The behaviour of the *atzR*–wt fusion was essentially as described (García-González *et al.*, 2005). In the absence of AtzR, expression was low under nitrogen excess, and greatly increased (~90-fold) under nitrogen limitation. In the presence of the AtzR-producing plasmid, expression was not altered in nitrogen-sufficient conditions, but was repressed under nitrogen limitation (15- or 20-fold, in the presence and in the absence of cyanuric acid respectively). None of the mutant constructs exhibited significant changes in expression relative to the wild type in the absence of AtzR. Similarly, activity was not altered in the presence of AtzR when grown in nitrogen-sufficient conditions. Expression from the *atzR*–ABS-1 and *atzR*–ABS-2 fusions was moderately increased (three- and fourfold, respectively, relative to the wild-type fusion) in nitrogen-limited medium containing cyanuric acid, while only a slight 1.5- to 2-fold effect was observed in the absence of the inducer. These results suggest that the contribution of the ABS-1 and ABS-2 sites to AtzR binding *in vivo* is most significant in the presence of cyanuric acid. In contrast, the *atzR*–ABS-3 fusion was derepressed fourfold in the absence of cyanuric acid, but less than twofold in its presence, consistent with the notion that contacts with ABS-3 *in vivo* occur preferentially when the inducer is not present.

Table 1. Expression of *atzR–lacZ* translational fusions containing mutations at the ABS in *P. putida* KT2442.

Plasmid	Fusion	*atzR* plasmid[a]	Growth conditions: Ammonium – CN	Serine – CN	Serine + CN[b]
			β-Galactosidase activity		
pMPO104	*atzR*–wt	No	15 ± 3	1340 ± 78	ND
		Yes	16 ± 2	91 ± 14	62 ± 13
pMPO145	*atzR*–ABS-1	No	17 ± 3	1516 ± 140	ND
		Yes	16 ± 4	129 ± 17	209 ± 9
pMPO149	*atzR*–ABS-2	No	12 ± 4	1252 ± 83	ND
		Yes	13 ± 3	147 ± 30	238 ± 9
pMPO151	*atzR*–ABS–3	No	19 ± 4	1400 ± 173	ND
		Yes	20 ± 3	392 ± 52	115 ± 9

a. Denotes the presence or absence of pMPO109, which produces AtzR from its own promoter.
b. Cyanuric acid (CN) (0.1 mM) was added to the growth medium.
Values are β-galactosidase activity (Miller units), and represent the average and standard deviation of at least three independent measurements.
ND, Not determined.

*Mutation of ABS-3 provokes signal-independent activation of P*atzDEF

The mutational analysis above showed that the ABS-3 mutation provokes an increase in P*atzDEF* activation levels in response to nitrogen limitation in the absence of cyanuric acid. Two explanations for this observation are feasible: (i) AtzR bound to the mutant promoter region exhibits enhanced sensitivity to the nitrogen limitation signal, and (ii) AtzR bound to the mutant promoter region is in a conformation that permits signal-independent activation. To distinguish between these two possibilities, we set out to determine whether AtzR activation of the ABS-3 mutant P*atzDEF* promoter region can occur in the absence of both cyanuric acid and the nitrogen limitation signal. For this, we exploited the fact that the nitrogen limitation status is communicated to AtzR via the PII signal transduction protein GlnK, and therefore, disruption of *glnK* renders AtzR unresponsive to nitrogen limitation (García-González *et al.*, 2009). Accordingly, expression of both the wild type (*atzD*–wt) and the ABS-3 mutant fusion (*atzD*–ABS-3) was analysed in a Δ*glnK P. putida* strain. Because both the Δ*glnK* strain MPO217 and our vector expressing *atzR* (pMPO109) are kanamycin resistant, a pMPO109-derived plasmid harbouring a tetracycline resistance gene, pMPO265, was used to provide AtzR in these β-galactosidase assays. In addition, as MPO217 is a glutamine auxotroph, to generate nitrogen excess conditions, 1 g l^{-1} glutamine was used as the nitrogen source, while serine-containing medium (nitrogen limitation conditions) was supplemented with 30 mg l^{-1} glutamine. Under these experimental conditions, the overall expression patterns of the *atzD*–wt fusion in *P. putida* KT2442 were for the most part comparable to those obtained in the conditions used above (Table 2). However, induced levels were decreased approximately threefold in nitrogen limitation conditions and 30–50% in nitrogen limitation with cyanuric acid (compare Fig. 4 and Table 2). Expression from the *atzD*–ABS-3 fusion was still similar to that from *atzD*–wt in all conditions, except for an approximately threefold increase in activation levels in nitrogen-limited medium lacking cyanuric acid.

When tested in a Δ*glnK* background, the β-galactosidase activity levels obtained with the *atzD*–wt fusion in the absence of AtzR were low in all conditions. When AtzR was provided, expression levels were low in the absence of cyanuric acid, irrespective of the nitrogen source, and were increased 13-fold in the presence of the inducer. As indicated above, the lack of response to nitrogen limitation in the Δ*glnK* background is due to the fact that GlnK is responsible for transmitting the nitrogen signal to AtzR (García-González *et al.*, 2009). On the other hand, the increased response to cyanuric acid in nitrogen excess is likely a consequence of increased AtzR concentration in these conditions, as deletion of *glnK* in *P. putida* provokes the constitutive expression of NtrC-dependent genes, including *atzR* (García-González *et al.*, 2009). The expression levels obtained with the *atzD*–ABS-3 mutant fusion in the absence of AtzR were similar to those in *atzD*–wt. However, in the presence of the regulator, the ABS-3 mutant displayed an approximately threefold increase in expression levels in the absence of cyanuric acid and a 50–70% increase in the presence of cyanuric acid relative to the wild-type strain, regardless of the nitrogen source. Since the ABS-3 mutation stimulates AtzR-dependent *atzDEF* activation in the absence of

Table 2. Effect of a *glnK* deletion on the expression of *atzD–lacZ* fusions harbouring the wild-type or the ABS-3 mutant binding site.

			Growth conditions			
			Nitrogen excess		Nitrogen limitation	
			– CN	+CN[b]	– CN	+ CN[b]
Strain	Fusion	*atzR* plasmid[a]	β-Galactosidase activity			
KT2442 (wild type)	*atzD*–wt	No	244 ± 34	236 ± 35	267 ± 56	348 ± 10
		Yes	282 ± 46	835 ± 126	3 900 ± 834	24 900 ± 3 410
	atzD–ABS–3	No	218 ± 43	209 ± 9	299 ± 50	358 ± 26
		Yes	312 ± 60	890 ± 140	10 400 ± 832	30 000 ± 3 260
MPO217 (Δ*glnK*)	*atzD*–wt	No	322 ± 38	351 ± 65	291 ± 39	282 ± 56
		Yes	737 ± 150	9 720 ± 1 380	678 ± 139	9 110 ± 1 860
	atzD–ABS–3	No	209 ± 28	221 ± 48	212 ± 41	200 ± 48
		Yes	1920 ± 489	16 900 ± 2 220	1 740 ± 123	13 700 ± 3 010

a. Denotes the presence or absence of pMPO265, which produces AtzR from its own promoter.
b. Cyanuric acid (CN) (0.1 mM) was added to the growth medium.
Glutamine (1 g l^{-1}) was used as a rich nitrogen source and 1 g l^{-1} serine with 30 mg l^{-1} glutamine was used as a poor nitrogen source. Cyanuric acid (CN) (0.1 mM) was added to the growth medium when required. Values are β-galactosidase activity (Miller units), and represent the average and standard deviation of at least three independent measurements.

cyanuric acid and in conditions in which the nitrogen limitation signal either is not generated (Δ*glnK* mutant in nitrogen excess), or cannot be transduced to AtzR (Δ*glnK* mutant in nitrogen limitation), we conclude that the ABS-3 mutation promotes signal-independent activation of the *atzDEF* operon.

The ABS-3 subsite is a strong AtzR binding determinant in the absence of cyanuric acid

The *in vivo* results above indicate that the ABS subsites have distinct roles in P*atzDEF* regulation. These roles may correlate with differential interaction of AtzR with different subsites ABS subsites as a function of the presence or absence of inducing conditions. To address the contribution of the individual ABS subsites to AtzR binding *in vitro*, gel mobility shift assays were performed using pure AtzR-His_6 and the wild type and individual ABS subsite mutant promoter regions as probes. The results are shown in Fig. 5.

The behaviour of AtzR on the wild-type probe was essentially as described: AtzR bound the P*atzDEF* promoter region with similar affinity to form a single retarded complex both in the presence and in the absence of cyanuric acid, and the complex formed in the presence of cyanuric acid exhibited faster mobility than that formed in the absence of the inducer (Porrúa *et al*., 2007). In the absence of cyanuric acid, affinity for the ABS-3 mutant binding site was clearly reduced relative to the wild-type site (approximately sevenfold) and the complex formed migrated slightly faster than that on the wild-type probe (Fig. 5A). In contrast, affinity was only barely diminished (less than twofold) in the presence of the inducer and the complex mobility was indistinguishable from the wild type (Fig. 5B). These results confirm the relevance of the mutated positions to AtzR binding and are consistent with the observation that AtzR contacts with ABS-3 *in vitro* occur most prominently in the absence of the inducer (see Porrúa *et al*., 2007, and Figs 2 and 3).

Gel mobility shift assays were also performed using ABS-1 and ABS-2 mutant probes (Fig. 5C and D). An older AtzR-His_6 preparation was used for these assays, which resulted in an approximately twofold increase in the apparent K_d of AtzR for the wild-type promoter region. Nevertheless, the ABS-1 and ABS-2 mutations did not significantly affect AtzR binding, as the mobility of the complexes formed was indistinguishable from those formed with the wild-type probe both in the presence and in the absence of cyanuric acid, and affinity was largely unaffected. These results suggest that the ABS-1 and ABS-2 subsites are weak binding determinants that do not individually contribute to AtzR binding *in vitro* to a significant extent.

The ABS-3 mutation releases AtzR contacts with the ABS-3 subsite, but does not mimic the presence of cyanuric acid

In the gel mobility shift assays above, mobility of AtzR bound to the ABS-3 probe in the absence of cyanuric acid was somewhat faster than that of the complex formed with the wild-type probe, suggesting that the ABS-3 mutation may somehow alter the structure of the AtzR–DNA complex at the *atzR–atzDEF* promoter region. Mutations that provoke changes in DNA bending by LTTRs have been shown to affect the activation process (Akakura and

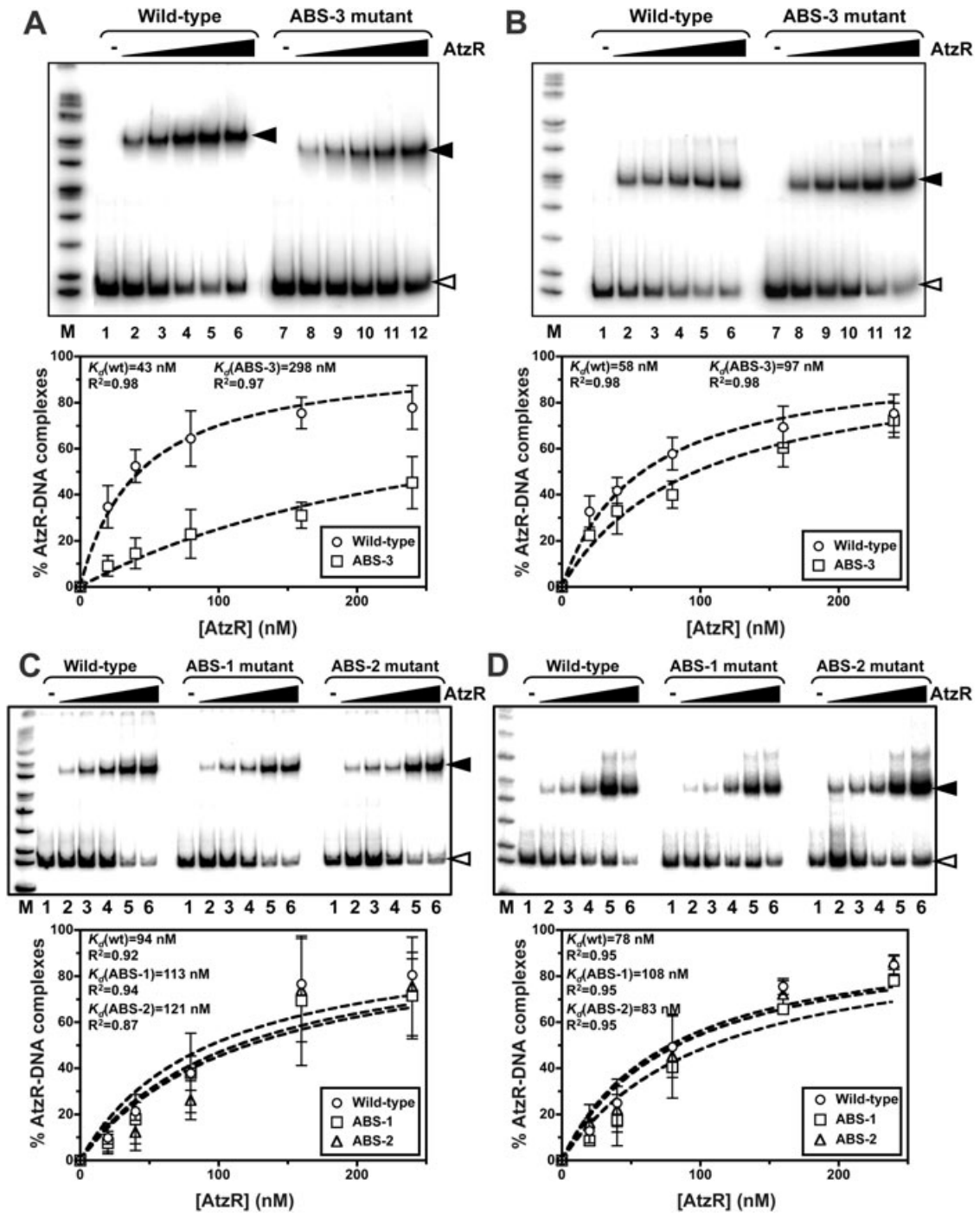

Fig. 5. Gel mobility shift analysis of AtzR binding to the ABS mutant binding sites.
A and B. Assays performed with the wild-type and ABS-3 mutant probes.
C and D. Assays performed with the ABS-1 and ABS-2 mutant probes.
Assays were carried out in the absence (A and C) or in the presence (B and D) of cyanuric acid. AtzR-His_6 concentrations were 0 (lanes 1 and 7), 20 (lanes 2 and 8), 40 (lanes 3 and 9), 80 (lanes 4 and 10), 160 (lanes 5 and 11) and 240 nM (lanes 6 and 12). AtzR–DNA complexes are indicated by closed arrowheads and naked probes are indicated by open arrowheads. Top of each panel: autoradiographs of gels representative of each experimental condition. Bottom: percentage of retarded probe plotted against AtzR-His_6 concentration. Curves represent the best-fitting rectangular hyperbola curves for each data set. The apparent dissociation constant (K_d) and *R*-squared values obtained from the fitted curves are indicated. Values and error bars represent the average and standard deviation of three to six independent experiments.

Winans, 2002). To test the effects of the ABS-3 mutation on AtzR-induced DNA bending, we performed circular permutation assays using digestion products of pMPO154, a pBend2-derived plasmid containing the ABS-3 mutant variant of the AtzR binding site, as probes for gel mobility shift assays. The relative mobilities of the AtzR–DNA complexes were plotted against the central co-ordinates of each promoter fragment and the data were fitted to second-degree polynomial curves in order to derive the bend centre and the average bending angle (Fig. 6), and the results were compared with those previously obtained with equivalent wild-type promoter fragments (Porrúa *et al.*, 2007). In the absence of cyanuric acid, the angle of the induced bend was somewhat diminished relative to the wild-type binding site (65° versus 71°), and the bend centre was displaced 4 bp away from the P*atzDEF* promoter, from position –45 to position –49 (Fig. 6A and C). In the presence of cyanuric acid the bend was also substantially relaxed relative to the wild-type promoter (Fig. 6B and C). However, poor fit of the relative mobility data to a symmetrical second-degree curve prevented the precise calculation of the bend centre and angle. This atypical behaviour of the AtzR–DNA complex and the fact that the lowest mobility fragment is centred within the ABS-3 subsite (position –31) suggests that a second bend may occur near the altered positions. Indeed, comparison of the PAGE mobility of DNA fragments harbouring the wild type or the mutant ABS-3 subsite suggests that the introduced mutations elicit a spontaneous low-angle bend (~20°) in the DNA strand (data not shown). The relevance of these changes in the features of the DNA bend in the ABS-3 probe relative to the wild type is difficult to evaluate. Nevertheless, it is evident that AtzR is still able to bend DNA at the mutant promoter region, and comparison of the relative mobility plots in the presence and in the absence of cyanuric acid reveals that the inducer exerts a comparable effect on AtzR-dependent DNA bending at the wild-type and mutant fragments. Thus, these results indicate that the AtzR–DNA complex formed at the ABS-3 mutant site in the absence of cyanuric acid is not equivalent to that formed in the presence of the inducer, and that this complex is still able to undergo an inducer-dependent rearrangement that is similar to that observed with the wild-type binding site.

In order to characterize further the changes in AtzR interaction with the *atzR–atzDEF* divergent promoter region provoked by the ABS-3 mutation, DNase I footprinting assays were performed using the bottom strand-labelled wild type and ABS-3 mutant promoter region as probes (Fig. 7). In the absence of cyanuric acid, the protection and hypersensitivity patterns of AtzR-His_6 on both probes were identical for the most part. However, contacts around the ABS-3 region were clearly altered in the

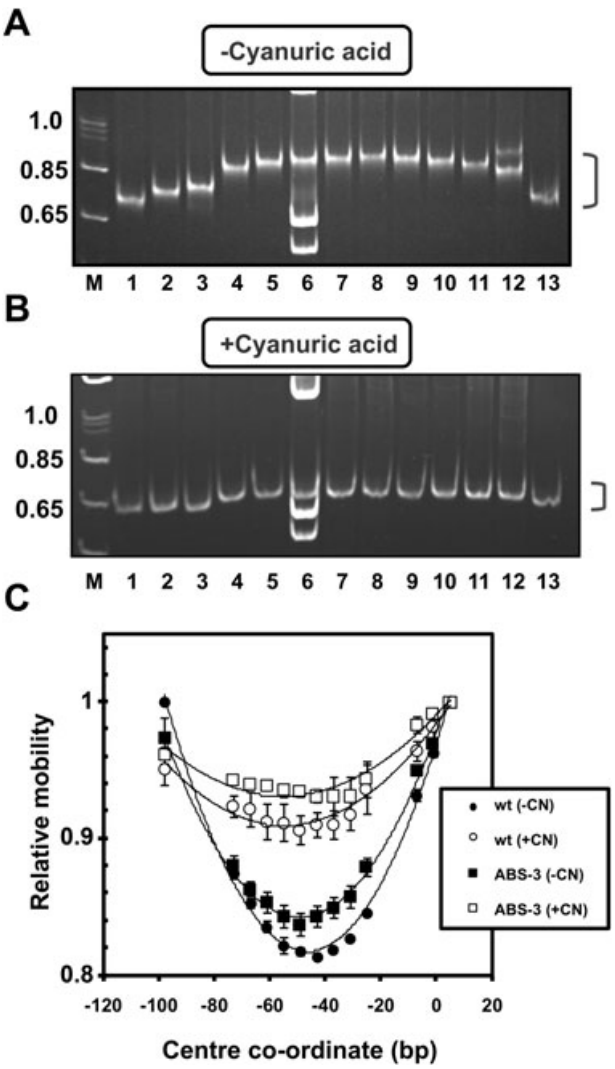

Fig. 6. Circular permutation analysis of AtzR binding to the ABS-3 mutant binding site.
A and B. Pictures of representative assays with the ABS-3 mutant promoter region in the absence (A) or in the presence (B) of cyanuric acid. The probes were pMPO154 digested with the following enzymes: MluI (lanes 1), BglII (lanes 2), NheI (lanes 3), SpeI (lanes 4), XhoI (lanes 5), DraI (lanes 6), EcoRV (lanes 7), PvuII (lanes 8), SmaI (lanes 9), StuI (lanes 10), NruI (lanes 11), SspI (lanes 12) and BamHI (lanes 13). M: DNA size marker. Relevant marker band sizes (in kb) are indicated on the left of each gel. Brackets denote the location of the AtzR–DNA complexes.
C. Relative mobility plots comparing the results obtained with the ABS-3 mutant binding site with those obtained with the wild-type site (Porrúa *et al.*, 2007) in the absence (–CN) and in the presence (+CN) of cyanuric acid.

mutant promoter region. As previously described (Porrúa *et al.*, 2007), in the absence of cyanuric acid, position –23 was fully protected and position –26 was partially protected in the wild-type probe. Protection at these two positions was not observed in the mutant promoter region. However, a new partially protected band occurred at position –25 (Fig. 7A and B), suggesting that, although binding

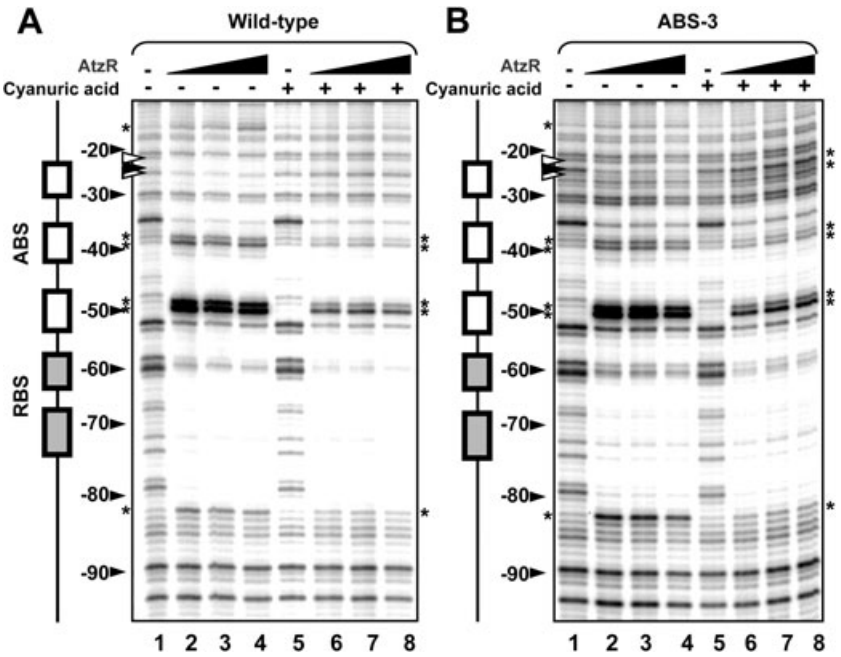

Fig. 7. DNase I footprinting analysis of the effect of the ABS-3 mutation on AtzR–DNA complexes.
A. AtzR binding to the wild-type *atzDEF* promoter region.
B. AtzR binding to the ABS-3 mutant promoter region.
AtzR-His_6 concentrations were 0 (lanes 1 and 5), 400 (lanes 2 and 6), 800 (lanes 3 and 7) and 1600 nM (lanes 4 and 8). Co-ordinates relative to the *atzDEF* transcriptional start are indicated. Grey and blank boxes denote the location of the RBS and ABS respectively. Open arrowheads designate positions –23 and –26. Closed arrowheads designate position –25. Asterisks indicate hypersensitive positions.

is severely reduced (Fig. 5A), the ABS-3 mutant site may still support some interactions with AtzR in the absence of cyanuric acid. In the presence of the inducer, protection at positions –23 and –26 was abolished in the wild-type probe, and hypersensitivity of bands around positions –40 and –50 was reduced. These traits have been shown to correlate with cyanuric acid-induced repositioning of AtzR and relaxation of the AtzR-induced DNA bend (Porrúa *et al*., 2007). Interestingly, a nearly identical footprint was obtained with the mutant promoter region in the presence of cyanuric acid (Fig. 7A and B), the only difference being two slightly hypersensitive positions at the mutation site (–25 and –27). This result is consistent with the notion that the inducer elicits a similar rearrangement in both promoter regions. Taken together, our *in vitro* analyses indicate that AtzR has reduced capacity to interact with the ABS-3 mutant subsite in the absence of cyanuric acid and document several small alterations in the AtzR–DNA complex formed on the mutant promoter region relative to that formed with the wild-type subsite. However, it is evident that inactivation of the ABS-3 subsite alone does not provoke a major rearrangement of the AtzR–promoter complex, nor does it affect the capacity of AtzR to respond to the presence of cyanuric acid by repositioning on its binding site region to form a complex that is almost indistinguishable from that formed at the wild-type promoter region.

Discussion

The results presented provide, along with those previously published (Porrúa *et al*. 2007; 2009), a detailed picture of the structure of the AtzR binding site at the *atzR–atzDEF* divergent promoter region. We have previously shown that the AtzR binding site is composed of a strong recognition motif, the RBS, harbouring the T-N_{11}-A LTTR conserved recognition element within an interrupted heptameric palindrome, which is centred at position –65 (relative to the P*atzDEF* promoter), and is required for AtzR binding, *atzDEF* activation and autorepression (Porrúa *et al*., 2007). A second region, the ABS, extends between the RBS and the P*atzDEF* promoter, overlapping the –35 box, and is required for activation (Porrúa *et al*., 2007) and autorepression (Porrúa *et al*., 2009). The structural details of the ABS were unknown, but we proposed that it is composed of three G-C-rich hexameric subsites that lie on the same face of the helix as the RBS (Porrúa *et al*., 2007) (Fig. 1). Our current findings are consistent with this prediction. Hydroxyl radical footprinting analysis indicates that AtzR interacts with DNA exclusively on one face of the helix (Figs 2 and 3). The protection pattern defines five patches of 3–4 bp exposed in the major groove facing AtzR. The exposed positions are enclosed within the proposed AtzR binding motifs (the two RBS half-sites and the three ABS subsites) and, as LTTRs interact with the DNA bases at their target sites through the major groove (Maddocks and Oyston, 2008), these regions likely represent the primary sites for sequence-specific interaction with the promoter region. The validity of this supposition is supported by the fact that substitutions at the exposed regions designed to decrease their similarity to the RBS yielded phenotypes consistent with diminished AtzR binding (Fig. 4 and Tables 1 and 2), and a decrease in AtzR binding affinity *in vitro* was directly

demonstrated for the ABS-3 subsite mutant (Fig. 5). The heptameric nature of the RBS half-sites is supported by the finding of a second functional AtzR binding site at the *orf98* promoter region immediately downstream from *atzR*, bearing an identical heptameric repeat (A.I. Platero and F. Govantes, unpublished). However, although we have defined our ABS subsites as hexamers, the relevance of all six positions to the function of the sites is not formally demonstrated. Considering the hydroxyl radical footprint data alone, a 'core' AtzR binding site may be defined as an array of tetrameric motifs exposed in five consecutive major grooves, with the sequence GTGC-N_7-GCAC-N_7-GTCG-N_6-GGCG-N_7-AGTG (positions unprotected in the hydroxyl radical footprint are underlined). In this simpler model, the perfect palindrome in motifs 1 and 2 corresponds to the RBS, and motifs 3, 4 and 5 correspond to the ABS subsites. Additional positions in the heptameric RBS half-sites or the hexameric ABS subsites may nevertheless play auxiliary roles in AtzR binding.

We have previously shown that cyanuric acid-dependent activation of the P*atzDEF* promoter occurs via a 'sliding dimer' mechanism (Porrúa *et al*., 2007), characterized by a relaxation of the AtzR-induced DNA bend and a shortening of the DNase I footprint in the presence of the inducer (Porrúa *et al*., 2007). The hydroxyl radical footprint results presented here indicate that such shortening is concomitant to a strong decrease in the contacts around the major groove that allows access to the ABS-3 subsite (Figs 2 and 3). This is consistent with a model in which AtzR responds to cyanuric acid by relocating its ABS-bound dimer from the ABS-2 and ABS-3 subsites to ABS-1 and ABS-2. A similar 'sliding dimer' mechanism has been demonstrated for OxyR (Toledano *et al*., 1994), OccR (Wang and Winans, 1995a,b), CbbR (van Keulen *et al*., 2003; Dubbs *et al*., 2004), ClcR (Macfall *et al*., 1997), BenM (Bundy *et al*., 2002) and GltC (Picossi *et al*., 2007), and CysB (Hryniewicz and Kredich, 1995), among others.

In vitro studies with mutant variants of the ABS subsites provide additional insight on the interactions of AtzR with the ABS in the absence and in the presence of cyanuric acid. Gel mobility shift assays indicate that the ABS-3 subsite is a major contributor to AtzR binding affinity only in the absence of inducer, while ABS-1 and ABS-2 do not significantly affect AtzR binding (Fig. 5). Interestingly, none of the mutations significantly affected the ability of AtzR to bend DNA or relax the DNA bend on the *atzDEF* promoter region in response to cyanuric acid, as judged from the mobility of the retarded complexes in gel mobility shift and circular permutation assays (Figs 5 and 7). These results implicate that remodelling of the AtzR–DNA complex is largely driven by interactions with the inducer, and cannot be mimicked by changes in the sequences for the individual subsites. This is in contrast with the results obtained with the OccR-activated *occQ* promoter, in which mutations at the ABS subsites have been shown to lock the OccR–DNA complex in a high-angle or low-angle conformation (Wang and Winans, 1995b; Akakura and Winans, 2002). Our results favour a model in which ABS-3 is a strong recognition element that promotes AtzR binding in an extended conformation to contact ABS-2 and ABS-3 (although ABS-2 appears to have a passive role in this interaction). The presence of cyanuric acid elicits a major rearrangement of AtzR to acquire a more compact conformation in which interaction with the stronger ABS-3 subsite is prevented and the DNA recognition elements are poised in the vicinity of the weaker ABS-1 and ABS-2 subsites (also see below). Crystallographic evidence of large conformational changes in response to effector binding has been obtained for the *Acinetobacter baylyi* LTTRs BenM and CatM, and a structural model depicting how these changes may elicit repositioning of the DNA-binding domains on DNA has been proposed (Ezezika *et al*., 2007; Craven *et al*., 2009).

We have used expression analysis of the P*atzDEF* promoter derivatives to examine the contribution of the individual ABS subsites to the regulation of the P*atzDEF* promoter *in vivo*. Activation in the presence of cyanuric acid was diminished in the ABS-1 and ABS-2 mutant fusions, while the ABS-3 mutation had little or no effect in the presence of the inducer (Fig. 4, Table 2). Similarly, P*atzR* repression was partly released in the ABS-1 and ABS-2 mutants in the presence of cyanuric acid, while the effect of the ABS-3 mutation in this condition was negligible. We conclude that, in accordance with the *in vitro* results, AtzR is located at the ABS-1 and ABS-2 subsites and has limited capacity to interact with ABS-3 in the presence of cyanuric acid *in vivo*. In addition, our results indicate that sequence-specific interaction with ABS-1 and ABS-2 is required for *atzDEF* activation and autorepression in the presence of the inducer (also see below).

The analysis of the ABS-3 mutant reveals yet another interesting trait of the activation process. In the absence of cyanuric acid, the ABS-3 mutation elicits inducer-independent P*atzDEF* activation (Fig. 4, Table 2), indicating that ABS-3 acts a repressor element. A similar increase in expression with mutants equivalent to ABS-3 has been shown for the CbbR-activated *cbb* operon of *Xanthobacter flavus* (van Keulen *et al*., 2003), the GltC-activated *gltAB* operon of *Bacillus subtilis* (Belitsky *et al*., 1995), and the Ccp-repressed *citB* promoter of *B. subtilis* (Kim *et al*., 2003). However, this phenotype was attributed to either increased availability of the –35 promoter element nearby the mutated motif (for *cbb* and *citB*), or a general improvement of the strength of the promoter (for *gltAB*), and no experimental evidence was shown in support of such mechanisms. In contrast, our *in vivo*

expression results show that inducer-independent activation due to inactivation of ABS-3 requires the integrity of the ABS-1 and ABS-2 subsites. Thus, the observed increase in P*atzDEF* expression is not the direct consequence of the release of contacts with ABS-3, but the result of interactions of AtzR with ABS-1 and ABS-2 when unanchored to ABS-3 (Fig. 4). We conclude that the high-affinity ABS-3 subsite of the *atzR–atzDEF* promoter region acts as a 'subunit trap' that lures AtzR into an inactive ABS-2- and ABS-3-bound conformation, thus preventing unwanted activation in the absence of inducer. This mechanism fits well with the results published for the *cbb*, *citB* and *gltAB* promoters (Belitsky *et al*., 1995; van Keulen *et al*., 2003; Kim *et al*., 2003), and may be of general applicability to other LTTR-regulated promoters.

AtzR is a unique LTTR in that it responds to two dissimilar signals, cyanuric acid and nitrogen limitation. We have recently shown that cyanuric acid is sensed directly by AtzR (Porrúa *et al*., 2007), while the nitrogen limitation signal is transmitted to AtzR by the PII protein GlnK, likely via protein–protein interactions (García-González *et al*., 2009). Nitrogen limitation activates *atzDEF* transcription by itself and together with cyanuric acid in an additive fashion (García-González *et al*., 2005), so that maximal expression levels are achieved in the presence of both signals. The molecular analysis of the nitrogen response of the *atzDEF* operon is limited by the fact that we cannot currently reproduce the nitrogen limitation signalling *in vitro*. However, the *in vivo* expression assays provide some interesting hints on the regulatory mechanisms involved. Several lines of evidence support the notion that AtzR interacts with all three ABS subsites *in vivo* during growth in nitrogen-limited medium lacking cyanuric acid. First, the ABS-1 and ABS-2 mutations fully abolished activation in response to nitrogen limitation (Fig. 4), indicating that AtzR must contact the ABS-1 and ABS-2 subsites to activate the P*atzDEF* promoter in this condition. Second, the ABS-3 mutation increased P*atzDEF* expression in response to nitrogen limitation to levels comparable to those achieved in the presence of both signals, and this increase in expression was dependent on the integrity of the ABS-1 and ABS-2 subsites (Fig. 4). Finally, partial derepression of the P*atzR* promoter in the ABS-3 mutant indicates that ABS-3 is a major binding determinant in nitrogen-limited medium not containing cyanuric acid (Table 1). The simplest explanation for these results is that AtzR is in a dynamic equilibrium between an inactive form that is tethered to ABS-3 and an active form, bound to ABS-1 and ABS-2. In this scenario, transition between the activating and non-activating conformations is driven by the affinity of AtzR for the individual ABS subsites, and mutations at the recognition elements for each form of AtzR may therefore alter the equilibrium towards the active or inactive conformation. We propose that interaction with GlnK under nitrogen limitation diminishes the affinity of AtzR for the ABS-3 subsite, and/or poses AtzR in a flexible conformation in which it can release contacts with ABS-3 and interact with ABS-1 and ABS-2 to activate transcription.

Simultaneous activation by nitrogen limitation and the presence of cyanuric acid yields the highest expression levels of the *atzDEF* operon. In these conditions, expression was unaltered by the ABS-3 mutation, and mutations at either ABS-1 or ABS-2 provoked a relatively modest decrease in expression, compared with the dramatic effect observed in the presence of nitrogen limitation alone (Fig. 4). Similarly, the AtzR–P*atzDEF* complex formed *in vitro* in the presence of cyanuric acid is essentially unaltered by mutational inactivation of the individual ABS subsites (Fig. 5). As discussed above, this reduced response to *cis*-acting mutations may reflect the cyanuric acid-induced rearrangement of the AtzR tetramer to a rigid compact conformation that poses the DNA-binding domains in the close vicinity of ABS-1 and ABS-2, thus facilitating AtzR interaction with these subsites, and negating interaction with ABS-3. In this scenario, the lack of competition between the two conformations of the protein may diminish the requirement for sequence-specific recognition of the ABS-1 and ABS-2 subsites. We note that cyanuric acid is sufficient to elicit the rearrangement of the AtzR–DNA complex *in vitro*, while full activation of the P*atzDEF* promoter *in vivo* requires the concerted action of both signals, even when AtzR is constitutively produced (García-González *et al*., 2005). Our preliminary results suggest that cyanuric acid uptake is nitrogen-regulated in *P. putida*, which may result in a low effective intracellular concentration of inducer under nitrogen excess (V. García-González and F. Govantes, unpublished). This notion is consistent with the increased induction by cyanuric acid in nitrogen-sufficient medium in the Δ*glnK* mutant (Table 2), as NtrC-activated genes are constitutively expressed in this background (García-González *et al*., 2009). However, the failure to achieve maximal P*atzDEF* expression in response to cyanuric acid in this mutant background strongly suggests that cyanuric acid and GlnK must somehow cooperate for AtzR to achieve the stable activating conformation required for the highest *atzDEF* expression levels.

Taken together, our results indicate that interaction of AtzR with the ABS at the *atzDEF* promoter region in the absence of stimuli is driven primarily by the high-affinity ABS-3 subsite. Interaction with ABS-3 strongly favours an inactive conformation of AtzR, thus preventing signal-independent activation. Transcriptional activation requires a transition in which AtzR releases contacts with the ABS-3 subsite to interact with ABS-1 and ABS-2. We propose that P*atzDEF* activation by AtzR occurs by two different mechanisms. First, a stable rearrangement of the

AtzR–DNA complex induced by cyanuric acid poses AtzR in the activating conformation. Such rearrangement is facilitated or stabilized further *in vivo* under nitrogen limitation conditions. Second, transient shifts in position of the ABS-bound dimer that favour contacts with the ABS-1 and ABS-2 subsites are promoted by a flexible conformation of AtzR that may occur in response to nitrogen limitation alone. Such transient interactions reflect a dynamic equilibrium between the inactive, ABS-3-bound form, and the active, ABS-1- and ABS-2-bound form of AtzR, and may thus be fostered by changes in the relative affinities of AtzR for the individual subsites.

Experimental procedures

Bacterial strains and growth conditions

Bacterial strains used in this work and their relevant genotypes are summarized in Table 3. Minimal medium containing 25 mM sodium succinate as the sole carbon source was used for *in vivo* gene expression analysis (Mandelbaum *et al.*, 1993). Nitrogen sources were ammonium chloride, L-glutamine or L-serine (1 g l^{-1}). When required, nitrogen-limited medium was supplemented with 30 mg l^{-1} glutamine. Luria–Bertani (LB) medium was used as rich medium (Sambrook *et al.*, 2000). Liquid cultures were grown in culture tubes or flasks with shaking (180–200 rpm) at 30°C or 37°C (for *P. putida* or *Escherichia coli* strains respectively). For solid media, Bacto-Agar (Difco, Detroit, Michigan) was added to a final concentration of 18 g l^{-1}. Antibiotics and other additions were used, when required, at the following concentrations: ampicillin (100 mg l^{-1}), kanamycin (20 mg l^{-1}), carbenicillin (500 mg l^{-1}), rifampicin (10 mg l^{-1}), chloramphenicol (15 mg l^{-1}), tetracyclin (5 mg l^{-1}) and 5-bromo-4-chloro-3-indoyl-β-D-galactopyranoside (X-gal) (25 mg l^{-1}). All reagents were purchased from Sigma-Aldrich.

Plasmid construction

Plasmids and oligonucleotides used in this work are summarized in Table 3. All DNA manipulations were performed according to standard procedures (Sambrook *et al.*, 2000). Restriction enzymes, DNA polymerases and T4 DNA ligase were purchased from Roche Applied Science. The Klenow fragment or T4 DNA polymerase was routinely used to fill-in recessed 3′ ends and trim protruding 3′ ends of incompatible restriction sites. Plasmid DNA preparation and DNA purification kits were purchased from Sigma-Aldrich, General Electric Healthcare or Macherey-Nagel and used according to the manufacturers specifications. Plasmid DNA was transferred to *E. coli* and *P. putida* strains by transformation (Inoue *et al.*, 1990) or by triparental mating (Espinosa-Urgel *et al.*, 2000). *E. coli* DH5α was used as a host in all cloning procedures.

Site-directed mutagenesis by overlap extension PCR was performed essentially as described (Aiyar *et al.*, 1996). The ABS-1, ABS-2 and ABS-3 mutant derivatives were generated using mutagenic oligonucleotide pairs HX1-rev/HX1-fwd, HX2-rev/HX2-fwd and HX3-rev/HX3-fwd, respectively, and external oligonucleotides (universal M13 forward and reverse primers) annealing to vector sequences. Plasmid pMPO108 was used as a template. The double mutant derivatives were generated similarly, using the single mutant promoters as templates and mutagenic oligonucleotides HX1+2-rev/HX1+2-fwd, HX3-rev/HX3-fwd and HX2+3-rev/HX2+3-fwd. To replace the wild-type fragment by the ones carrying the desired mutations, the final PCR products were digested with SphI and HindIII and ligated into SphI- and HindIII-digested pMPO202, resulting in the *atzD–lacZ* fusion plasmids pMPO144, pMPO148, pMPO150, pMPO169, pMPO170 and pMPO171. Similarly, the SphI- and HindIII-digested products of the ABS-1, ABS-2 and ABS-3 reactions were ligated into SphI- and HindIII-digested pMPO104 to yield the *atzR–lacZ* fusion plasmids pMPO145, pMPO149 and pMPO151. The ABS-3 fragment was also cloned into SalI-digested pBend2 to yield the circular permutation plasmid pMPO154. A SmaI fragment of pUTminiTn*5*-Tc was cloned into SmaI-linearized pMPO109 to produce pMPO265.

β-Galactosidase assays

Steady-state β-galactosidase assays were used to examine the expression of the wild type and mutant *atzD–lacZ* and *atzR–lacZ* fusions in *P. putida* KT2442 or its Δ*glnK* derivative MPO217. Preinocula of bacterial strains harbouring the relevant plasmids were grown to saturation in minimal medium under nitrogen-sufficient conditions (ammonium chloride or L-glutamine, 1 g l^{-1}) and cells were then diluted in minimal medium containing the appropriate nitrogen sources (1 g l^{-1} ammonium chloride or L-glutamine for nitrogen excess; 1 g l^{-1} L-serine, supplemented when required with 25 g l^{-1} L-glutamine for nitrogen limitation). Diluted cultures were shaken for 16–24 h to mid-exponential phase (OD_{600} = 0.25–0.5). Growth was then stopped and β-galactosidase activity was determined from SDS- and chloroform-permeabilized cells as previously described (Miller, 1992).

Gel mobility shift assays

AtzR-His_6 was purified from the overproducing strain NCM631 harbouring pMPO135 and pIZ227 by nickel affinity chromatography as previously described (Porrúa *et al.*, 2007). Probes containing the wild type or the ABS-1, ABS-2 or ABS-3 mutant AtzR binding sites were obtained by PCR using plasmids pMPO202, pMPO144, pMPO148 or pMPO150, respectively, as templates and primers oligo-UP and Seq-BamHI, annealing to flanking pMPO200 vector sequences. The PCR products were subsequently digested with ClaI and gel purified. DNA fragments were strand-specifically labelled by filling in the 5′ overhanging ends using the Klenow fragment in a reaction mixture containing [α-^{32}P]-dCTP. Unincorporated nucleotides were removed using the MSB Spin PCRapace kit (Invitek).

AtzR–DNA complexes were formed at room temperature in 20 µl of reactions containing 10 ng of the probe, 100 µg ml^{-1} salmon sperm DNA, 250 µg ml^{-1} BSA and increasing amounts of purified AtzR-His_6 (0–240 nM) in binding buffer (35 mM Tris acetate, 70 mM potassium acetate, 20 mM ammonium acetate, 2 mM magnesium acetate, 1 mM

Table 3. Bacterial strains, plasmids and oligonucleotides used in this work.

Bacterial strain	Genotype/phenotype	Reference/source
E. coli DH5α	ϕ80d*lacZ*ΔM15 Δ(*lacZYA-argF*)U169 *recA*1 *endA*1 *hsdR*17 (r_k^- m_k^+) *supE*44 *thi*-1 *gyrA relA*1	Hanahan (1983)
E. coli NCM631	*hsdS gal* λDE3:*lacI lacUV5:gen1*(T7 RNA polymerase) Δ*lac* linked to Tn*10*	Govantes *et al.* (1996)
P. putida KT2442	mt-2 *hsdR*1 (r^- m^+) Rif^r	Franklin *et al.* (1981)
P. putida MPO217	mt-2 *hsdR*1 (r^- m^+) Rif^r Δ*glnK*::Km^r	García-González *et al.* (2009)
Plasmid	**Genotype/phenotype**	**Reference/source**
pBend2	Vector for circular permutation analysis. Ap^r.	Kim *et al.* (1989)
pIZ227	pACYC184 containing *lacI*^{q} and the T7 lisozyme gene. Cm^r	Govantes *et al.* (1996)
pMPO104	*atzR–lacZ* translational fusion in pMPO200 containing the wild-type promoter sequence. Ap^r	García-González *et al.* (2005)
pMPO108	630 bp fragment containing the *atzR–atzDEF* divergent promoter region, cloned in pBluescript II KS (+). Ap^r	García-González *et al.* (2005)
pMPO109	*atzR* coding sequence and promoter region cloned in pKT230. Km^r	García-González *et al.* (2005)
pMPO135	pET23b plasmid derivative overexpressing AtzR-His_6. Ap^r	Porrúa *et al.* (2007)
pMPO141	pBend2-based plasmid for circular permutation analysis of the AtzR binding site. Ap^r	Porrúa *et al.* (2007)
pMPO144	*atzD–lacZ* translational fusion in pMPO200 containing the ABS-1 mutant sequence. Ap^r	This work
pMPO145	*atzR–lacZ* translational fusion in pMPO200 containing the ABS-1 mutant sequence. Ap^r	This work
pMPO148	*atzD–lacZ* translational fusion in pMPO200 containing the ABS-2 mutant sequence. Ap^r	This work
pMPO149	*atzR–lacZ* translational fusion in pMPO200 containing the ABS-2 mutant sequence. Ap^r	This work
pMPO150	*atzD–lacZ* translational fusion in pMPO200 containing the ABS-3 mutant sequence. Ap^r	This work
pMPO151	*atzR–lacZ* translational fusion in pMPO200 containing the ABS-3 mutant sequence. Ap^r	This work
pMPO154	pMPO141-derived plasmid containing the ABS-3 mutant sequence. Ap^r	This work
pMPO169	*atzD–lacZ* translational fusion in pMPO200 containing the ABS-1 and ABS-2 mutant sequences. Ap^r	This work
pMPO170	*atzD–lacZ* translational fusion in pMPO200 containing the ABS-1 and ABS-3 mutant sequences. Ap^r	This work
pMPO171	*atzD–lacZ* translational fusion in pMPO200 containing the ABS-2 and ABS-3 mutant sequences. Ap^r	This work
pMPO200	Broad-host-range *lacZ* translational fusion vector, based on pBBR1MCS-4. Ap^r	García-González *et al.* (2005)
pMPO202	*atzD–lacZ* translational fusion in pMPO200 containing the wild-type promoter sequence. Ap^r	García-González *et al.* (2005)
pMPO265	pMPO109 derivative with the Km resistance changed to tetracycline. Tc^r	This work
pRK2013	Helper plasmid used in conjugation. Km^r Tra^+	Figurski and Helinski (1979)
pUTminiTn*5*-Tc	Delivery plasmid for miniTn*5*-Tc insertion. Ap^r Tc^r	de Lorenzo *et al.* (1990)

Oligonucleotide	Sequence (5′ to 3′)
M13 forward	GTTTTCCCAGTCACGAC
M13 reverse	ACGGGATAACAATTTCA
oligo-UP	GTATTCCAGATCCTGGACGC
Seq-BamHI	GATCCCCAGGGCTGTGGCAAG
Seq-ClaI	CGATGTAATGAAGAAAGCGT
HX1-fwd	GCACCAGTTAGTCTGGAAAAAGGCG
HX1-rev	CGCCTTTTTCCAGACTAACTGGTGC
HX2-fwd	GTCGGAAAAAGTACGCAGTCAAGTG
HX2-rev	CACTTGACTGCGTACTTTTTCCGAC
HX3-fwd	CGGCAGTCAACACAGAGGGCGGCG
HX3-rev	CGCCGCCCTGCTGTGTTGACTGCCG
HX1+2-fwd	GTCTGGAAAAAGTACGCAGTCAAGTG
HX1+2-rev	CACTTGACTGCGTACTTTTTCCAGAC
HX2+3-fwd	GTACGCAGTCAACACAGCAGGGCGGCG
HX2+3-rev	CGCCGCCCTGCTGTGTTGACTGCGATC

Oligonucleotide positions altered from the template sequences are underlined.

calcium chloride, 1 mM DTT, 5% glycerol, pH 7.9) for 20 min. Reactions were stopped with 3 μl of loading buffer [0.125% w/v bromophenol blue, 0.125% w/v xylene cyanol, 10 mM Tris HCl (pH 8), 1 mM EDTA, 30% glycerol] and samples were separated on a 5% polyacrylamide native gel in Tris-borate-EDTA buffer at 4°C. Dried gels were exposed to a phosphoscreen and analysed using the ImageQuant software (Amersham), as previously described (Porrúa *et al*., 2007). The fraction of probe bound to AtzR was plotted against the concentration of AtzR-His_6. The data from three to six independent repeats of each assay were fitted to one-site binding (rectangular hyperbola) curves using the non-linear regression function of GraphPad Prism software, with B_{max} (maximal binding) set to 100% of bound probe, and the equations obtained were used to derive the apparent dissociation constant (K_d) for each data set.

Hydroxyl radical footprinting

Hydroxyl radical footprinting assays based on the procedure of Tullius *et al*. (1987), with some modifications, were used to map AtzR binding to DNA with high resolution. For these experiments, DNA probes were strand-specifically radiolabelled by PCR amplification using an unlabelled oligonucleotide and a T4 polynucleotide kinase 5′ end radiolabelled oligonucleotide. PCR reactions were performed with pMPO202 as a template and primers pair Seq-BamHI and Seq-ClaI and the products were separated on a 5% polyacrylamide gel and purified. AtzR–DNA complexes were formed for > 20 min at room temperature in 50 μl of reactions in binding buffer (10 mM Tris-HCl, pH 8; 100 mM sodium chloride; 1 mM EDTA; 1 mM dithiothreitol; 0.5% glycerol) containing 4×10^4 cpm DNA probe, 400 nM AtzR, 0.5 μg of salmon sperm DNA and 0.1 μg of BSA. Hydroxyl radicals were produced by mixing equal volumes of freshly prepared Fe(II)-EDTA solution [0.2 mM ammonium-iron (II) sulphate, 0.4 mM EDTA], 20 mM sodium ascorbate and 0.6% hydrogen peroxide. The cleavage reaction was initiated by adding 9 μl of this reagent mixture. After 2 min incubation at room temperature, 14.7 μl of STOP solution (1.5 M sodium acetate, pH 7.0; 41 mM thiourea; 0.68 mg ml^{-1} tRNA) and 187 μl of 96% ethanol were added. The mixture was incubated overnight at –20°C, the precipitate was recovered by centrifugation, rinsed with 70% ethanol, dried and resuspended in 5 μl of loading buffer (80% v/v formamide, 10 mM sodium hydroxide, 1 mM EDTA, 0.1% w/v bromophenol blue, 0.1% w/v xylene cyanol). Finally, samples were boiled for 5–10 min and run on a 6% polyacrylamide–6 M urea denaturing sequencing gel together with a Maxam and Gilbert G+A ladder. Gels were processed and analysed as described above.

DNase I footprinting

DNase I footprinting assays with AtzR were performed essentially as described (Porrúa *et al*., 2007). Probes for DNase I footprinting were obtained by PCR amplification of the DNA fragment of interest as described for gel mobility shift assays. Binding reactions were performed in binding buffer (35 mM Tris acetate, 70 mM potassium acetate, 20 mM ammonium acetate, 2 mM magnesium acetate, 1 mM calcium chloride, 1 mM dithiothreitol, 5% glycerol, 100 μg ml^{-1} salmon sperm DNA, 250 μg ml^{-1} BSA, pH 7.9) containing 20 ng of the radiolabelled probe and 0–1.6 μM AtzR in a final volume of 20 μl. After 20 min incubation at room temperature, partial digestion of the DNA was initiated by the addition of 1 μl of an empirically determined dilution (typically 10^{-2} to 10^{-3}) of a DNase I stock solution (10 U ml^{-1}, Roche Diagnostics). Incubation was continued for 30 additional seconds and reactions were stopped by the addition of 5 μl of stop buffer (1.5 M sodium acetate, pH 5.2; 130 mM EDTA; 1 mg ml^{-1} salmon sperm DNA; 2.4 mg ml^{-1} glycogen). DNA was subsequently ethanol precipitated, resuspended in 5 μl of loading buffer (0.125% w/v bromophenol blue, 0.125% w/v xylene cyanol, 20 mM EDTA, 95% v/v formamide) and separated by gel electrophoresis on a 6% polyacrylamide–6 M urea denaturing sequencing gel. A sequencing reaction was performed with the Sequenase 2.0 kit (USB) using primer Seq-ClaI and was run in parallel as a size marker. Gels were processed and analysed as described above.

Circular permutation analysis

Circular permutation analysis was performed to assess DNA bending by AtzR using the pBend2 vector as previously described (Kim *et al*., 1989; Porrúa *et al*., 2007). A plasmid containing the wild type or the ABS-3 mutant AtzR binding site (pMPO141 or pMPO154 respectively) was subjected to single digestion with the following restriction enzymes: MluI, BglII, NheI, SpeI, XhoI, DraI, EcoRV, PvuII, SmaI, StuI, NruI, SspI and BamHI. The mixed products of each digestion were cleaned of other components of the reactions with the MSB Spin PCRapace kit (Invitek) and then a binding reaction was performed using 0.6 μM AtzR and 1 μg of each digestion mixture as a probe. Assay conditions were identical to those for the gel mobility shift assay, except for the absence of competing DNA. Samples were separated on a 5% polyacrylamide native gel in Tris-borate-EDTA buffer at 4°C. Finally, gels were stained with 5 mg l^{-1} ethidium bromide and DNA bands were visualized by UV fluorescence. The relative mobility of AtzR–DNA complexes in three independent experiments was plotted as a function of the co-ordinate of the DNA fragment centre and fitted to a second-degree polynomial curve. The bending centre was calculated as the co-ordinate corresponding to the minimal relative mobility in the fitted curve. We used the minimal relative mobility in the fitted curve as an estimation of the relative mobility of a complex containing the bend at its centre (μ_M/μ_E), and this value was used to calculate the bend angle α using the equation $(\mu_M/\mu_E) = \cos(\alpha/2)$ (Thompson and Landy, 1988), as previously described (Porrúa *et al*., 2007).

Acknowledgements

We wish to thank Guadalupe Martín and Nuria Pérez for technical help, Victoria Shingler for enlightening discussion of the results, and all members of the Govantes and Santero laboratories for their insights and helpful suggestions. This work was supported by Grants BIO2004-01354 and BIO2007-63754 (Ministerio de Educación y Ciencia, Spain), and a fellowship from the I3P (CSIC/Ministerio de Educación y Ciencia, Spain) programme, awarded to O.P.

References

Aiyar, A., Xiang, Y., and Leis, J. (1996) Site-directed mutagenesis using overlap extension PCR. *Methods Mol Biol* **57:** 177–191.

Akakura, R., and Winans, S.C. (2002) Mutations in the *occQ* operator that decrease OccR-induced DNA bending do not cause constitutive promoter activity. *J Biol Chem* **277:** 15773–15780.

Belitsky, B.R., Janssen, P.J., and Sonenshein, A.L. (1995) Sites required for GltC-dependent regulation of *Bacillus subtilis* glutamate synthase expression. *J Bacteriol* **177:** 5686–5695.

Bundy, B.M., Collier, L.S., Hoover, T.R., and Neidle, E.L. (2002) Synergistic transcriptional activation by one regulatory protein in response to two metabolites. *Proc Natl Acad Sci USA* **99:** 7693–7698.

Craven, S.H., Ezezika, O.C., Haddad, S., Hall, R.A., Momany, C., and Neidle, E.L. (2009) Inducer responses of BenM, a LysR-type transcriptional regulator from *Acinetobacter baylyi* ADP1. *Mol Microbiol* **72:** 881–894.

Dubbs, P., Dubbs, J.M., and Tabita, F.R. (2004) Effector-mediated interaction of CbbRI and CbbRII regulators with target sequences in *Rhodobacter capsulatus*. *J Bacteriol* **186:** 8026–8035.

Espinosa-Urgel, M., Salido, A., and Ramos, J.L. (2000) Genetic analysis of functions involved in adhesion of *Pseudomonas putida* to seeds. *J Bacteriol* **182:** 2363–2369.

Ezezika, O.C., Haddad, S., Clark, T.J., Neidle, E.L., and Momany, C. (2007) Distinct effector-binding sites enable synergistic transcriptional activation by BenM, a LysR-type regulator. *J Mol Biol* **367:** 616–629.

Figurski, D.H., and Helinski, D.R. (1979) Replication of an origin-containing derivative of plasmid RK2 dependent on a plasmid function provided in *trans*. *Proc Natl Acad Sci USA* **76:** 1648–1652.

Franklin, F.C., Bagdasarian, M., Bagdasarian, M.M., and Timmis, K.N. (1981) Molecular and functional analysis of the TOL plasmid pWWO from *Pseudomonas putida* and cloning of genes for the entire regulated aromatic ring meta cleavage pathway. *Proc Natl Acad Sci USA* **78:** 7458–7462.

García-González, V., Govantes, F., Porrúa, O., and Santero, E. (2005) Regulation of the *Pseudomonas* sp. strain ADP cyanuric acid degradation operon. *J Bacteriol* **187:** 155–167.

García-González, V., Jiménez-Fernández, A., Hervás, A.B., Canosa, I., Santero, E., and Govantes, F. (2009) Distinct roles for NtrC and GlnK in nitrogen regulation of the *Pseudomonas* sp. strain ADP cyanuric acid utilization operon. *FEMS Microbiol Lett* **300:** 222–229.

Govantes, F., Molina-Lopez, J.A., and Santero, E. (1996) Mechanism of coordinated synthesis of the antagonistic regulatory proteins NifL and NifA of *Klebsiella pneumoniae*. *J Bacteriol* **178:** 6817–6823.

Govantes, F., Porrúa, O., García-González, V., and Santero, E. (2009) Atrazine biodegradation in the lab and in the field: enzymatic activities and gene regulation. *Microbial Biotechnol* **2:** 178–185.

Hanahan, D. (1983) Studies on transformation of *Escherichia coli* with plasmids. *J Mol Biol* **166:** 557–580.

Hryniewicz, M.M., and Kredich, N.M. (1995) Hydroxyl radical footprints and half-site arrangements of binding sites for the CysB transcriptional activator of *Salmonella typhimurium*. *J Bacteriol* **177:** 2343–2353.

Inoue, H., Nojima, H., and Okayama, H. (1990) High efficiency transformation of *Escherichia coli* with plasmids. *Gene* **96:** 23–28.

van Keulen, G., Ridder, A.N., Dijkhuizen, L., and Meijer, W.G. (2003) Analysis of DNA binding and transcriptional activation by the LysR-type transcriptional regulator CbbR of *Xanthobacter flavus*. *J Bacteriol* **185:** 1245–1252.

Kim, J., Zwieb, C., Wu, C., and Adhya, S. (1989) Bending of DNA by gene-regulatory proteins: construction and use of a DNA bending vector. *Gene* **85:** 15–23.

Kim, S.I., Jourlin-Castelli, C., Wellington, S.R., and Sonenshein, A.L. (2003) Mechanism of repression by *Bacillus subtilis* CcpC, a LysR family regulator. *J Mol Biol* **334:** 609–624.

de Lorenzo, V., Herrero, M., Jakubzik, U., and Timmis, K.N. (1990) Mini-Tn*5* transposon derivatives for insertion mutagenesis, promoter probing, and chromosomal insertion of cloned DNA in gram-negative eubacteria. *J Bacteriol* **172:** 6568–6572.

MacFall, S., Parsek, M.R., and Chakrabarty, A.M. (1997) 2-Chloromuconate and ClcR-mediated activation of the *clcABD* operon: *in vitro* transcriptional and DNase I footprint analyses. *J Bacteriol* **179:** 3655–3663.

Maddocks, S.E., and Oyston, P.C. (2008) Structure and function of the LysR-type transcriptional regulator (LTTR) family proteins. *Microbiology* **154:** 3609–3623.

Mandelbaum, R.T., Wackett, L.P., and Allan, D.L. (1993) Mineralization of the *s*-triazine ring of atrazine by stable bacterial mixed cultures. *Appl Environ Microbiol* **59:** 1695–1701.

Miller, J.H. (1992) *A Short Course in Bacterial Genetics: A Laboratory Manual*. Cold Spring Harbor, NY: Cold Spring Harbor Laboratory Press.

Muraoka, S., Okumura, R., Ogawa, N., Nonaka, T., Miyashita, K., and Senda, T. (2003) Crystal structure of a full-length LysR-type transcriptional regulator, CbnR: unusual combination of two subunit forms and molecular bases for causing and changing DNA bend. *J Mol Biol* **328:** 555–566.

Picossi, S., Belitsky, B.R., and Sonenshein, A.L. (2007) Molecular mechanism of the regulation of *Bacillus subtilis gltAB* expression by GltC. *J Mol Biol* **365:** 1298–1313.

Porrúa, O., García-Jaramillo, M., Santero, E., and Govantes, F. (2007) The LysR-type regulator AtzR binding site: DNA sequences involved in activation, repression and cyanuric acid-dependent repositioning. *Mol Microbiol* **66:** 410–427.

Porrúa, O., García-González, V., Santero, E., Shingler, V., and Govantes, F. (2009) Activation and repression of a σ^N-dependent promoter naturally lacking upstream activation sequences. *Mol Microbiol* **73:** 419–433.

Sambrook, J., Russell, D.W., and Russell, D. (2000) *Molecular Cloning, a Laboratory Manual*. Cold Spring Harbor, NY: Cold Spring Harbor Laboratory Press.

Schell, M.A. (1993) Molecular biology of the LysR family of transcriptional regulators. *Annu Rev Microbiol* **47:** 597–626.

Thompson, J.F., and Landy, A. (1988) Empirical estimation of protein-induced DNA bending angles: applications to

lambda site-specific recombination complexes. *Nucleic Acids Res* **16:** 9687–9705.

Toledano, M.B., Kullik, I., Trinh, F., Baird, P.T., Schneider, T.D., and Storz, G. (1994) Redox-dependent shift of OxyR–DNA contacts along an extended DNA-binding site: a mechanism for differential promoter selection. *Cell* **78:** 897–909.

Tropel, D., and van der Meer, J.R. (2004) Bacterial transcriptional regulators for degradation pathways of aromatic compounds. *Microbiol Mol Biol Rev* **68:** 474–500.

Tullius, T.D., Dombroski, B.A., Churchill, M.E., and Kam, L. (1987) Hydroxyl radical footprinting: a high-resolution method for mapping protein–DNA contacts. *Methods Enzymol* **155:** 537–558.

Wang, L., and Winans, S.C. (1995a) High angle and ligand-induced low angle DNA bends incited by OccR lie in the same plane with OccR bound to the interior angle. *J Mol Biol* **253:** 32–38.

Wang, L., and Winans, S.C. (1995b) The sixty nucleotide OccR operator contains a subsite essential and sufficient for OccR binding and a second subsite required for ligand-responsive DNA bending. *J Mol Biol* **253:** 691–702.